Biochimica et Biophysica Acta, 591 (1980) 187—197
© Elsevier/North-Holland Biomedical Press

BBA 47851

INTRACELLULAR OXYGEN MEASUREMENTS OF MOUSE LIVER CELLS USING QUANTITATIVE FLUORESCENCE VIDEO MICROSCOPY

DOUGLAS M. BENSON, JAMES A. KNOPP and IAN S. LONGMUIR

Department of Biochemistry, North Carolina State University, Raleigh, NC 27650 (U.S.A.)

(Received November 8th, 1979)

Key words: Oxygen assay; Fluorescence video microscopy; (Mouse liver)

Summary

Our currently developed fluorescence video microscope can measure fluorescence intensities with an error of ±1.5% of full scale in 65 536 different positions of a microscope field. With a video frame freeze acquisition time of 33 ms, time-dependent changes of this order of time or slower can be followed. Using cells which have absorbed pyrene-1-butyrate to an intracellular concentration of 0.05 to 1 mM, the changes in fluorescence intensity with oxygen concentration are easily measured. The spatial resolution for data collection is 0.5 μm when a 54X objective is used. The individual Stern-Volmer quenching constants of each individual pixel were measured for agar slices and mouse liver cells treated with pyrenebutyric acid. The distribution of quenching constants for agar follows a normal curve about a mean value of $16 \cdot 10^{-4}$ torr^{-1}. The data for mouse liver cells gave a non-normal distribution of quenching constants with a mean value of $18 \cdot 10^{-4}$ torr^{-1}. The greater spread of the data from cells is interpreted as evidence for a real biological variation in the solubility coefficient of oxygen in different locations within the cell. In all the cells examined, this distribution has been observed to be non-random and appears to be associated with specific cell structures.

Introduction

Oxygen is well known as a general quencher of fluorescence emission of many compounds. The evidence by Vaughan and Weber [1] demonstrated that at physiologically important pO_2 values the fluorescence of pyrenebutyric acid was significantly quenched, due to the long fluorescence lifetime of 140 ns and the efficiency of the quenching process (approx. 100%). Their results suggested that pyrenebutyric acid could be used to measure oxygen

concentrations under physiological conditions. We presented the first demonstration that pyrenebutyric acid was easily absorbed by cells and that gradients of fluorescence intensity could be observed [2]. Others have extended this procedure to other systems [3—11].

Since the observed variations in fluorescence intensities of pyrenebutyric acid within the cells were greater than could be expected for any possible oxygen gradients, it was obvious that the procedure must be modified so that, at every single measuring point within the cell, the ratio of fluorescence intensities in the absence and presence of oxygen must be determined. In this way the fractional quenching could be established. Furthermore, local environmental variations in viscosity and oxygen solubility may occur within the cell so that a range in the Stern-Volmer quenching constants would be expected. Data are presented in this report on the measurement of the Stern-Volmer quenching constants at different points within the cell to test for the spatial variability.

The quenching of fluorescence by oxygen has been shown experimentally to obey a first-order Stern-Volmer quenching equation: $F_0/F = 1 + K_q[O_2]$ where F_0 and F are the fluorescence intensities in the absence and presence of oxygen, K_q is the Stern-Volmer quenching constant which in this case is the diffusion-controlled rate constant for collisions between oxygen molecules and excited states and $[O_2]$ is the concentration of molecular oxygen in solution. We have previously shown that the quenching process reflects the concentration rather than the activity of oxygen [12]. For physiologically important samples, it is customary to express this last term as pO_2, the partial pressure of oxygen in the gas phase which is in equilibrium with the aqueous phase. The equation now becomes: $F_0/F = 1 + \alpha K_q pO_2$ where α is the Bunsen solubility coefficient. In heterogeneous systems such as living cells, variations in oxygen solubility are certainly to be expected. Therefore, the slope of the plot of the reciprocal of reduced fluorescence versus pO_2 represents the product of the solubility and the quenching constant. From an empirical point of view, this distinction is of no importance in determining the oxygen at a particular point in a sample. However, this distinction is of importance in the interpretation of variations in αK_q within the field of measurement, be it a cell or a tissue slice. The question is raised as to whether these differences reflect variations in oxygen solubilities or microviscosities from region to region within the specimen.

Materials and Methods

1-Pyrenebutyric acid was prepared as previously described [12]. All other chemicals were reagent grade. Oxygen was medical grade and nitrogen showed no trace of oxygen by Scholander analysis.

Liver cells were isolated from mice (International Cancer Research, 7—13 weeks old) by EDTA digestion [13] and suspended in 100 mM phosphate, 17 mM EDTA buffer (pH 7.4). Pyrenebutyric acid was introduced into the cells by suspending 0.5 ml of packed cells in 10 ml of 10 μM pyrenebutyric acid in phosphate-EDTA buffer. This procedure resulted in an intracellular pyrenebutyric acid concentration of approx. 200 μM. After several washings

the cell suspension was diluted and a drop was placed on a coverslip which was secured in an airtight lucite chamber.

Agar, which was used as a control, was prepared by dissolving agar in 200 μM pyrenebutyric acid and phosphate-EDTA buffer to make a 1% solution. The solutions were heated to 80°C and small drops were placed on coverslips and allowed to cool.

The pO_2 in the lucite chamber was varied by flushing with N_2, air, or O_2 gas. These gases were humidified by bubbling through the phosphate-EDTA buffer, and flowmeters were used to insure a constant flowrate of 200 ml/min for each gas. This flowrate resulted in an equilibration time of less than 5 min as determined by the change in intensity. The chamber was designed to be attached to the stage of a Leitz Ortholux II fluorescence microscope.

The excitation system consisted of a 150 watt Xenon high pressure arc (Osram XBO 150/1), a 10 cm H_2O filter, a 340 interference filter, an electronic shutter, a vertical illuminator, and a Leitz 54X objective. The electronic shutter was used to reduce the illumination time and minimize photodecomposition. The fluorescence image was collected by the same objective, passed through a 420 nm interference filter, and was projected on the vidicon of a Silicon Intensified Target television camera (Cohu 4300).

The analog signals from the camera were stored on a single frame video memory (CVI MS200) for immediate analysis and on a videotape recorder (Javelin 400X) for permanent record. The acquisition time of a single frame was 33 ms. These signals were converted to digital form at 8-bit resolution by a modified video bandwidth compressor (CVI model 260). The sampling process gave a maximum data set per frame of 256×256 or 65 536 pixels. The maximum sampling rate was 4096 pixels/s. A Challenger II-P microcomputer (Ohio Scientific Instruments) controlled the shutter, the frame freeze, and the video processor. The microcomputer also performed the calculations necessary for data reduction, and presented the data in graphical form using an X-Y digital plotter (Hi Plot, Houston Instruments).

The standard deviations of the intensities were independent of the intensity. The mean standard deviation for a single frame was 2 for a range of intensities from 0 to 225 (full scale). The mean standard deviation for the intensities of an image averaged over 32 frames was 5 for the same intensity range. Normal sampling protocol was to average 4 frames, each being sampled 4 times, for a total of 16 measurements/pixel.

Quenching constants were calculated for each pixel by first subtracting the dark current and taking the ratio of the fluorescence intensity under nitrogen to the fluorescence intensity for all other pO_2 levels. These ratios were then compared to the pO_2 by linear regression and the slopes were stored, providing a matrix of αK_q values. Values were rejected if the correlation coefficient was less than 0.9 or if the F_0 intensity was less than 32 (1/8 full scale). This selection eliminated less than 5% of the pixels within the cell boundary.

Cells from mouse liver were mixed with 1 mM PBA solutions at pH 9 for 5 min. The treated cells were centrifuged and washed with buffer. The cells were lysed by three freeze-thaw cycles and centrifuged at $30\,000 \times g$. The supernatants were brought to pH 12 and passed through 0.2 μm Millipore filters. The resultant solutions were extracted with chloroform at pH 4 and

re-extracted back into the aqueous phase with 5% NaOH. The concentrations of pyrenebutyric acid were determined by absorption spectroscopy.

Results

As control media, agar was chosen because of the expected homogeneity of composition and the relative rigidity, which minimizes the diffusion of pyrenebutyric acid during measurements. Fluorescence intensity measurements were made on freshly prepared droplets which were equilibrated with either oxygen, nitrogen, or air. Samples which showed evidence of movement or loss of water were discarded. While the agar samples showed variation in the fluorescence intensities across the microscope field, due mainly to the uneven illumination, there was no corresponding pattern in the calculated quenching constants. The data for the agar samples, shown in Fig. 1, give an average quenching constant of $15.6 \cdot 10^{-4}$ torr^{-1} with a standard deviation of $1.5 \cdot 10^{-4}$ torr^{-1}. There was little variation from sample to sample.

When pyrenebutyric acid is mixed with cells, it is rapidly absorbed as previously noted [2]. The concentration of free pyrenebutyric acid dropped to less than 1% of the initial value, and the mean intracellular pyrenebutyric acid concentration was calculated assuming that all of the pyrenebutyric acid was located within the packed cell volume. The total data set of the quenching constants for 11 difference cell experiments are summarized in Fig. 1. The calculated mean value for αK_q was $18.1 \cdot 10^{-4}$ torr^{-1} with a standard deviation of $5.2 \cdot 10^{-4}$ torr^{-1}. The observed mean quenching constant is very close to that obtained in aqueous buffer $(20 \pm 2) \cdot 10^{-4}$ torr^{-1} [12] and is higher than that obtained in agar. The spread of the quenching constant data for the cells taken as a whole is much greater than that for agar. The standard deviations of the quenching constants for each individual cell are also greater than that observed for agar. Table I summarizes the data of the individual experiments. During the course of the equilibration with different gases, cells would occasionally either move or dry and thereby increase in diameter due to flat-

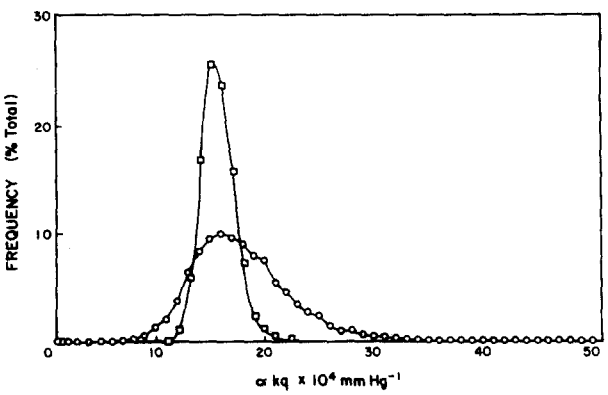

Fig. 1. The frequency distribution of the Stern-Volmer quenching constants of all data shown in Table I. The number of pixels having a particular αK_q divided by the total number of pixels is plotted versus αK_q for mouse liver cells (○) and agar slices (□).

TABLE I

SUMMARY OF OXYGEN QUENCHING CONSTANTS IN MOUSE LIVER CELLS AND AGAR DROPLETS

The integrated intensity values of αKq are those calculated by summing the entire intensity map for each different pO_2 (O_2, N_2, and air). The pixel values of αKq are those calculated point by point. Because some point calculations gave poor correlation coefficients (<0.9), these data points were not included in the data given here, and the percent of the data points presented are given as % data calculated. The mean values were calculated giving equal weight to each experiment.

Sample	Expt. No.	Quenching constant = αKq					
		Integrated αKq	Pixel αKq	S.D.	Mode	Number of pixels	% Data calculated
Cells	1	18.3	18.9	8.6	15	1234	96
	2	16.9	17.6	3.7	17	1169	90
	3	25.3	21.9	3.5	20	493	33
	4	20.7	20.8	4.8	20	1096	87
	5	21.0	20.2	4.6	18	788	72
	6	19.6	18.9	4.3	19	805	92
	7	17.7	18.2	3.5	17	1894	92
	8	14.2	14.8	3.9	14	1717	84
	9	18.9	19.8	3.7	18	1807	88
	10	15.1	15.5	2.9	15	2031	99
Mean		18.8	18.9				
S.D.		3.0	2.3				
S.E.		0.91	0.69				
1% Agar	1	15.7	15.7	1.6	15	2048	100
	2	15.4	15.4	1.4	15	2048	100
Mean		15.6	15.6				
S.D.		0.21	0.21				
S.E.		0.15	0.15				

tening. Such experiments were considered invalid. When the calculations were attempted on the data from such invalid experiments, the standard deviations were quite large, an order of magnitude greater than that seen in Table I, and definite skewed quenching constant distribution profiles were observed.

In contrast to the data from the agar sample, the fluorescence intensity values from the cells showed a wider range of zero to full scale. Initial measurements, using a video tape recorder for intermediate analog data storage, gave wide variations in quenching constants and an apparent correlation between quenching constants and fluorescence intensity [13]. Refinements in data collection and analysis have minimized the noise input, giving the quenching constant distribution shown in Fig. 1. Fig. 2 compares the fluorescence intensity map (2 a) of a single cell with the quenching constant map (2 b) as calculated for the same cell. There is no relationship between the fluorescence intensity and the calculated quenching constant. There is a marked increase in the quenching constants around the periphery of the cell. We continue to observe a minimum of fluorescence intensity from the area of the cell where the nucleus is located, supporting our previous observations that pyrenebutyric acid appears to be excluded from the nucleus.

The lack of correlation between fluorescence intensity and quenching con-

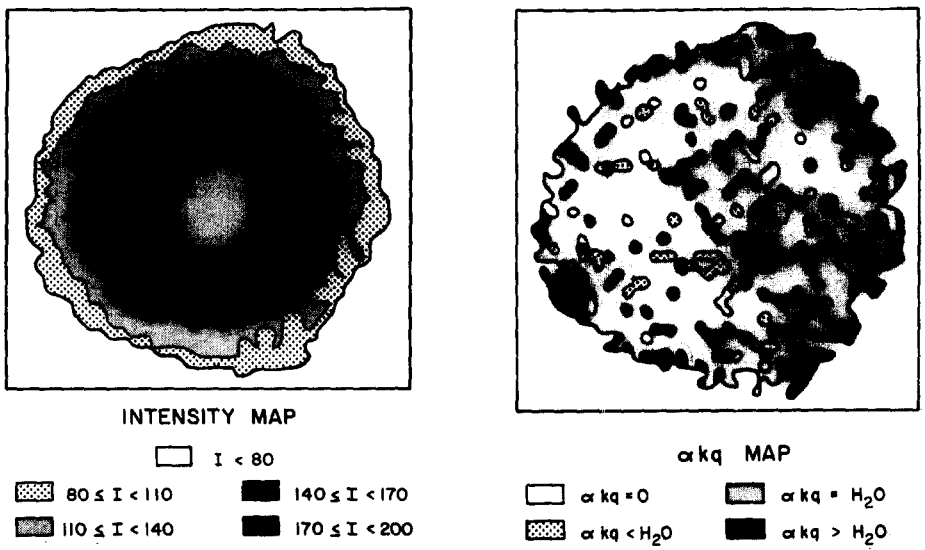

Fig. 2 (a) A contour map of the spatial distribution of the fluorescence intensity under nitrogen. The relative fluorescence intensity from the pyrenebutyric acid-treated liver cell was measured at 420 nm when excited by incident illumination with 340 nm light. Full scale is 255 or $2^8 - 1$. (b) A contour map of the spatial distribution of the Stern-Volmer quenching constant. The individual pixel intensities of the pyrenebutyric acid-treated cell under N_2, O_2, and air were fitted to the Stern-Volmer equation, and the best fit slopes were calculated to give the quenching constants. Those values which gave a low correlation coefficient (<0.9) were assigned a value of zero and represent 4% of the total pixels for the cell. Values of 1 to $14 \cdot 10^{-4}$ $torr^{-1}$ are shown as less than that for water and represent 6% of the total pixels. Values of 15 to $24 \cdot 10^{-4}$ $torr^{-1}$ are shown as equal to that in water and represent 71% of the total. Those values greater than $24 \cdot 10^{-4}$ $torr^{-1}$ are shown as greater than that for water and represent 19%.

stant is further demonstrated in Fig. 3. The quenching constant data set taken from the cell shown in Fig. 2 was plotted versus the fluorescence intensity in the absence of oxygen (F_0), pixel by pixel. There is no dependence of the quenching constant upon the fluorescence intensity. Linear regression analysis

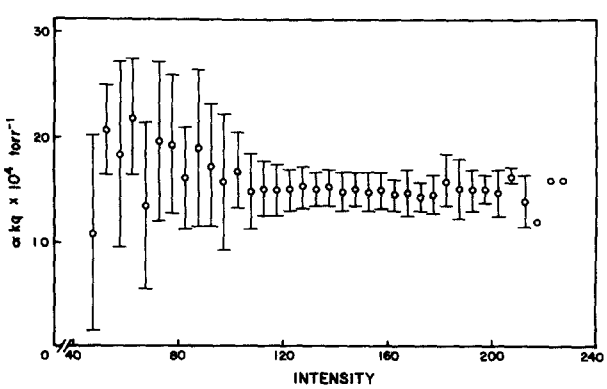

Fig. 3. Correlation between quenching constants and fluorescence intensity. The data shown in Fig. 2 are plotted as the pixel αK_q versus the pixel intensity under N_2 for all the pixels within the cell periphery. The data shown in Fig. 2 were analyzed by grouping the pixels together by pixel intensity when the pyrenebutyric acid-treated cell was under N_2 and calculating the mean and standard deviation of the αK_q corresponding to these pixels.

of these points gave a slope of −0.03 with a correlation coefficient of −0.205.

Previous work [12] had shown that all the cell organelles with the exception of the nucleus take up pyrenebutyric acid, and our subsequent experiments on cell cytosol showed that there was no significant difference in the amount of pyrenebutyric acid found in the soluble and insoluble fractions from the cell homogenates.

Discussion

The spatial resolution of the video detection system is limited by the nature of the video signal. We used only one of the two interlace frames which gave 256 lines or rows per frame. The sampling video digitizer was set to give a maximum of 256 steps or columns across the frame so that a single frame was divided into 256^2 or 65 536 pixels. When a 54X objective is used, the pixel center-to-center distance is 0.5 μm. With a 10X objective this distance becomes 3 μm. These values represent the maximum resolution obtainable, and in practice a lower resolution is applicable due to either spatial averaging of the intensities or by limiting the number of pixels per frame by equi-distance spacing.

The resolution in the measurement of pO_2 is limited by the standard error in the intensity readings. The standard deviations of the intensities of a large number of pixels were found to be independent of intensity. The mean standard deviation for a single frame from the video frame freeze was determined to be 2, of which 0.5 is due to the analog-digital converter of the video digitizer and 1.5 is most likely due to a timing uncertainty in the sampling circuits. The mean standard deviation from several frames of the same image was found to be 5. For one frame of an image of 100 × 100 pixels, the shutter is open for 167 ms, the frame is stored in 33 ms, and the data is converted from analog to digital form in 9 s. To sample the same image four times per frame for four frames requires 140 s. Assuming a fluorescence quenching constant of $20 \cdot 10^{-4}$ torr^{-1} and the sampling protocol we employed, one would expect a resolution of ± (12—15) torr for a pO_2 of 0—200 torr. It is possible to decrease the standard error in pO_2 by increasing the number of samples, either temporally or spatially.

The location of pyrenebutyric acid within the cell is still not exactly determined. Our previous report [12] gave evidence for the high affinity of pyrenebutyric acid for the microsomal fraction. Certainly because of the hydrophobic nature of the pyrene ring, it would be expected to be buried within membrane structures. Similar reasoning was used by Edwards et al. [10] and Wong et al. [6] in their studies with pyrenebutyric acid in which they presumed pyrenebutyric acid was located in the membrane structure. However, pyrenebutyric acid will also bind tightly to proteins and, in particular, serum albumins. Our previous sucrose gradient measurements, as well as the cytosol distribution experiments, indicate that, with the exception of the nucleus, pyrenebutyric acid should be found in all components within the cell, although to differing degrees.

As the intracellular pyrenebutyric acid concentration was raised to 1 to 2 mM, excimer fluorescence was observed. Under these conditions, we observed

decreases in the quenching constant as measured by 420 nm emission. With our current instrumentation, an intracellular pyrenebutyric acid concentration of 25 μM gave a half maximum signal. From this lower limit, until excimer formation occurred, there was no effect of pyrenebutyric acid concentration on the observed mean intracellular quenching constant. The preferred pyrenebutyric acid concentration is 100 μM. This is well below the excimer concentration minimum, is in the region where there is no effect on cellular respiration [8], and provides more than adequate signal.

Initial experiments showed a possible correlation between fluorescence intensity at a particular point within a cell and the quenching constant calculated for that position [13]. With improvements by the reduction of the noise and the time between collection of analog data and its conversion into digital form, this correlation disappeared. As clearly seen in Figs. 2 and 3, there is no relationship between fluorescence intensities and observed quenching constants. The mean quenching constants of $(18 \pm 4) \cdot 10^{-4}$ torr^{-1} agree well with the value of 16 to 18 $\cdot 10^{-4}$ torr^{-1} as calculated from the data by Edwards et al. [10] who used hamster kidney cell lines, and are slightly higher than that which we reported for whole cell as determined macroscopically $[(13 \pm 2) \cdot 10^{-4}$ torr$^{-1}]$. This value also agrees well with the value determined in aqueous solution as noted above.

In the re-examination of the fluorescence intensity maps which were first reported by us [2], we find that not only is there spatial variation in the fluorescence intensity due to variations in pyrenebutyric acid concentrations within the cell, but also due to variation of the quenching constants within the cell. The quenching constant distribution experiments with agar slices demonstrates the

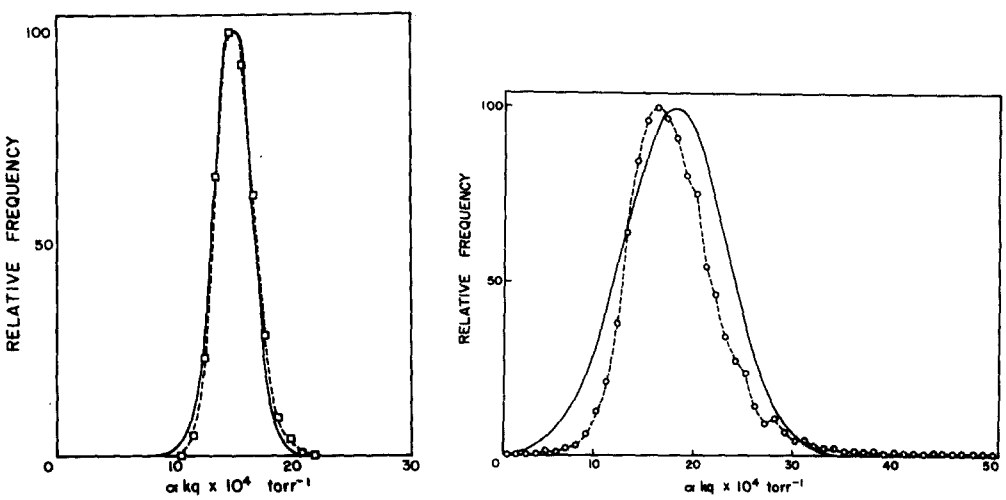

Fig. 4. The frequency distribution of the Stern-Volmer quenching constants for agar slices. The same data as shown in Fig. 1 for agar slices is shown by the dotted line. The calculated distribution, assuming a normal distribution with the same mean and standard deviation as the experimental data, is shown as the solid line.

Fig. 5. The frequency distribution of the Stern-Volmer quenching constants for a single cell. The same data as shown in Fig. 1 for mouse liver cells is shown by the dotted line. The calculated distribution, assuming a normal distribution with the same mean and standard deviation as the experimental data, is shown as the solid line.

maximum random variation to be expected in these values. The standard deviation of 4096 different pixels was 10% of the mean. In addition, the frequency distribution of the quenching constants follows the normal distribution curve quite well. Fig. 4 shows the distribution of all 4096 pixels and, for comparison, the normal distribution curve as calculated using the mean and standard deviation of the actual data. In contrast, the standard deviation of the cell quenching constants is approximately 25% of the mean value. Furthermore, the frequency distribution of the quenching constants for all 13 000 pixels of all the cells does not fit a normal distribution. Fig. 5 shows the comparison between the observed distribution and that calculated from the mean and standard deviation for a single cell. Attempts were made to fit either the leading edge or the trailing edge with normal curves, but only one side at a time could be made to fit. No single, normal curve was found which would fit both sides. The distribution of quenching constants for each cell was tested separately to determine if there were fits to a normal distribution. Two of the ten cells tested had distribution curves somewhat resembling a normal distribution, but the fit was not as close as for the agar experiments.

We conclude that the range in quenching constants is greater than that expected on the basis of noise or uncertainty in the data and must be attributed to the presence of more than one class of quenching constants within the cells. This variation cannot be attributed to variations in pyrenebutyric acid concentrations because the quenching constants have been shown to be independent of the concentration and intensity (Fig. 3). As noted in the Introduction, the calculated quenching constant is a product of the solubility of oxygen and the diffusion-controlled collision rate constant. This is a consequence of using partial pressure rather than concentration of oxygen as the independent variable. The diffusion-controlled rate constant is a function of the diffusion constant which includes the viscosity, the collision efficiency, the unquenched fluorescence lifetime, and parameters related to molecular dimensions. The data of Burleson [11] shows little change in the fluorescence lifetime when pyrenebutyric acid is absorbed in cells and cellular membranes. If the collision efficiency and the diffusion of oxygen is the same, then the K_q term would be expected to be invariant throughout the cell. This would imply that the variations observed must be due primarily to variations in the solubility of oxygen within the cell. For our experiments, this represents biological variability of at least 3- to 5-fold in oxygen solubility. Since we are examining a two-dimensional projection of a three-dimensional structure, with some degree of averaging, the true hetereogeneity must be greater than this.

A closer examination of Fig. 2b, which shows the distribution of αK_q across the cell, shows regions of quenching constants less than that in water, equal to that in water, and greater than that in water. When pyrenebutyric acid is bound to proteins, the pyrene ring would become less accessible to oxygen. This would decrease the collision efficiency and give a lower quenching constant as shown by the measurements of pyrenebutyric acid bound to bovine serum albumin [1]. Consequently, regions where the quenching constant is significantly lower than in water should be and were observed. Early work on the solubility and diffusion of oxygen in lipids [14] suggested that regions of lipids may be the

origin of the high quenching constant values. To test this hypothesis, the integrated intensity measurements were made of pyrenebutyric acid in single isolated adipocytes, which are essentially one large lipid droplet surrounded by a thin layer of cytoplasm and cell membrane. The fluorescence intensity of these cells was characterized as a bright ring coincident with the cytoplasm, indicating that pyrenebutyric acid does not completely enter the lipid phase. We observed a mean quenching constant of up to three times that determined for pyrenebutyric acid in liver cells. We would like to suggest that the regions of high quenching constants within the liver cell periphery are due to the burying of the pyrene ring in lipid droplets. Therefore, as cells vary in lipid content, the high end of the quenching constant distribution curve will vary, giving rise to differences in the mean αK_q for cells. It should be noted that pyrenebutyric acid in organelles high in membrane such as microsomes and mitochondria has previously been shown to have quenching constants less than that in water. These organelles cannot be the origin of the observed high quenching constants.

In summary, the quenching constant map for mouse liver cells shows that most of the area has approximately the same value as for water. Approximately 20% of the area in the cell exhibits significantly lower quenching constants. This could be due to either protein binding of the pyrenebutyric acid or low oxygen solubility. Approximately 10% of the area of the cell exhibits significantly higher quenching constants, expected for regions of lipid droplets. The distribution of αK_q will depend upon the location and relative amount of these different contributions and may indeed be dynamic in time. Great caution must be exercised when dealing with measurements at this level of magnification. When groups of cells such as tissue slices are measured at lower magnification, the variations in αK_q become less due to spatial averaging, thus simplifying measurements of oxygen gradients. Under these latter conditions, it becomes meaningful to speak of a single value for cellular αK_q which is represented by our integrated intensity measurements in Table I.

In addition, we have shown that it is possible to measure quantitatively the fluorescence intensity at different points of an image and to perform calculations on such measurements. Obviously, the instrumentation is not limited to measurements of in vivo oxygen concentrations using pyrenebutyric acid but can be applied to any problem which requires both spatial resolution and quantitation of fluorescence signals.

Acknowledgements

This paper is a contribution from the Department of Biochemistry, School of Agriculture and Life Sciences and School of Physical and Mathematical Sciences. Paper No. 6200 of the Journal Series of the North Carolina Agricultural Research Service, Raleigh, NC 27650. It was supported in part by Grant No. HL-16828 from the National Institutes of Health.

The authors thank Ms. Patricia Campbell for her technical assistance.

References

1 Vaughan, W.M. and Weber, G. (1970) Biochemistry 9, 464—473
2 Knopp, J.A. and Longmuir, I.S. (1972) Biochim. Biophys. Acta 279, 393—397

3 Cheng, S., Thomas, J.K. and Kulpa, C.F. (1974) Biochemistry 13, 1135—1139
4 Kohen, E., Salmon, J.M., Kohen, C. and Bengtsson, G. (1974) Exp. Cell Res. 89, 105—110
5 Geiger, M.W. and Turro, N.J. (1975) Photochem. Photobiol. 22, 273—276
6 Wong, M., Kulpa, C.F. and Thomas, J.K. (1976) Biochim. Biophys. Acta 426, 711—722
7 Jöbsis, F.F., Mitnichk, M.H. and Snow, T.R. (1976) in Second International Symposium on Oxygen Transport to Tissue (Grote, J., Reneau, D. and Thews, G., eds.), pp. 47—54, Plenum Press, New York
8 Snow, T.R. and Jöbsis, F.F. (1976) Biochim. Biophys. Acta 440, 36—44
9 Mitnick, M.H. and Jöbsis, F.F. (1976) J. Appl. Physiol. 41, 593—597
10 Edwards, H.E., Thomas, J.K., Burleson, G.R. and Kulpa, C.F. (1976) Biochim. Biophys. Acta 448, 451—459
11 Burleson, G.R., Kulpa, C.F., Edwards, H.E. and Thomas, J.K. (1978) Exp. Cell Res. 116, 291—300
12 Longmuir, I.S. and Knopp, J.A. (1976) J. Appl. Physiol. 41, 598—602
13 Benson, D.M. (1977) Master's Thesis, North Carolina State University, Raleigh, N.C.
14 Davidson, D., Eggleton, P. and Foggie, P. (1952) Q. J. Exp. Physiol. 37, 91—105